JOURNAL OF MATERIALS SCIENCE 24 (1989) 749–755

Complex impedance and admittance of a silver-conducting glass

AKIRA DOI
Department of Materials, Nagoya Institute of Technology, Nagoya 466, Japan

From the analysis of complex impedance and admittance data of $(AgI)_{75}(Ag_4P_2O_7)_{25}$ glass, an Ag^+-ion conductor, it was revealed that the sample can be approximated by a series RC_1 circuit at high temperature, with the capacitor C_1 arising from the charge-carrier depleted region near the anode which develops as conduction proceeds, and by a parallel RC_2 circuit at low temperature, with the capacitor C_2 arising from the saturated value for ionic polarization of, say, the silver–iodine pairs as well as from the relaxation effect of the Ag^+ ions for conduction. The C_1 and C_2 values were found to be almost temperature-independent at peak frequencies of the distorted semicircles in respective complex planes, with the ratio C_1/C_2 as large as 10^4.

1. Introduction

Complex impedance and admittance measurements have frequently been made as a useful technique for investigating various phenomena which occur when a glass is biassed by an a.c. electric field. The purpose of this work is to apply this technique to one of the Ag^+-ion conductors, the $(AgI)_{75}(Ag_4P_2O_7)_{25}$ glass, and to obtain further insight into ionic-conduction related phenomena in glass. Experimental details have been presented elsewhere [1] and will not be given here.

2. Results and discussion

Suppose the applied field is given by

$$E^* = E_0 \exp[-j(\omega t - Kr)] \quad (1)$$

where ω is the angular frequency and K the propagation constant. In order to describe correctly the phase lags of various responses to the stimulus, E^*, the complex admittance Y^* and complex impedance Z^* should be written as

$$Y^* = G - jB \qquad G, B \geqslant 0 \quad (2)$$

and

$$Z^* = Z_1 + jZ_2 \quad Z_1, Z_2 \geqslant 0 \quad (3)$$

The corresponding complex dielectric constant is, then,

$$\varepsilon^* = \varepsilon_1 + j\varepsilon_2 \quad \varepsilon_1, \varepsilon_2 \geqslant 0 \quad (4)$$

Figs 1 and 2 illustrate some of the complex admittance data of the glass measured in the frequency range from 5 to 5×10^5 Hz. As is apparent, the locus of the B–G plots with increasing temperatures completes the distorted semicircle which terminates at the origin. It is well known that the minima of B other than the origin, which we term "the spikes", correspond to d.c. conductivities. Fig. 3 shows the Arrhenius plots of σ_{dc} thus determined from the spikes in the complex admittance plane, as well as from the spikes in the complex impedance plane, as discussed below.

The a.c. conductivity, σ_{ac}, when defined using the sample thickness d and the electrode area s, as

$$\sigma_{ac} = (d/s)G \quad (5)$$

was found to decrease from the plateau ($\leftrightarrow \sigma_{dc}$) at frequencies less than that for the spike [1]. This low-frequency dispersion was attributed [2] to a decrease in the effective field for conduction within a glass bulk by the development of the charge-carrier depleted region (CDR) near the anode as conduction proceeds. Once the CDR is formed, it is possible that the sample is approximated by a series RC_1 circuit composed of the resistor, R, of the glass bulk and the capacitor, C_1, of CDR, as shown in Fig. 4. Provided R and C_1 are frequency independent, we should find a semicircle in the B–G plane which intersects the G axis at the origin and at $1/R$ ($= s\sigma_{dc}/d$) (Fig. 4c), in partial agreement with our observation. The term "partial" means that our semicircles are flattened to some extent, with the centre of the circle shifted downwards in the fourth quadrant. The ratio of the short length to the long length of the distorted semicircle, b/a, lies within 0.72 ± 0.04. The distortion of this sort would arise from the frequency dependences of R and C_1. As CDR develops, Z_1 ($= R$) is no longer constant, and increases with decreasing frequencies, while Z_2 ($= 1/\omega C_1$) increases below the ω^{-1} dependency by the growing values for C_1 [1]. Hence, we observe a distorted semicircle by different frequency dependences of B ($= Z_2/(Z_1^2 + Z_2^2)$) and G ($= Z_1/(Z_1^2 + Z_2^2)$).

The peak of an ideal semicircle corresponds to the angular frequency, ω_c, at which an equality $\omega_c RC_1 = 1$ holds. Provided this relation holds true even for the distorted semicircles, we can estimate the values for C_1. Those thus estimated are found to be almost temperature-independent (Table I), except at high temperatures where deviation from linearity was

0022–2461/89 $03.00 + .12

TABLE I Information obtained from complex admittance data; b/a is the ratio of the short to long lengths of the distorted semicircle, RC_1 and C_1 are respectively the time constant and the capacitance of the series RC_1 circuit as estimated at the peak of the semicircle using the relation $\omega_c RC_1 = 1$, σ_{dc} is the d.c. conductivity found at the spike, and $\pi\sigma_{dc}/\omega_c$ is the charge flowed into the cathode by conduction per unit applied field and per half-cycle of the angular frequency, ω_c, at the peak

	−99.9° C	−90.0° C	−79.9° C	−69.8° C	−59.9° C	−40.2° C	−20.0° C	+1.0° C	+19.5° C	+36.2° C
b/a	0.680	0.710	0.718	0.702	0.682	0.712	0.756	0.763	0.748	0.696
RC_1 (sec)	1.33×10^{-2}	5.32×10^{-3}	2.27×10^{-3}	9.95×10^{-4}	5.31×10^{-4}	1.99×10^{-4}	7.24×10^{-5}	4.19×10^{-5}	2.65×10^{-5}	1.59×10^{-5}
C_1/s ($\times 10^{-7}$ F cm^{-2})	6.24	6.01	5.53	6.37	6.77	6.59	5.36	5.16	5.57	4.45
σ_{dc} (Ω^{-1} cm^{-1})	2.84×10^{-6}	6.83×10^{-6}	1.47×10^{-5}	3.87×10^{-5}	7.70×10^{-5}	2.00×10^{-4}	4.47×10^{-4}	7.44×10^{-4}	1.27×10^{-3}	1.69×10^{-3}
$\pi\sigma_{dc}/\omega_c$ ($\times 10^{-7}$ F cm^{-1})	1.18	1.14	1.05	1.21	1.28	1.25	1.02	0.98	1.05	0.84

TABLE II Information obtained from complex admittance data; b/a is the ratio of short to long lengths of the distorted semicircle, RC_2 and C_2 are respectively the constant and the capacitance of the parallel RC_2 circuit as estimated at the peak of the semicircle using the relation $\omega_c RC_2 = 1$, and σ_{dc} is the d.c. conductivity found at the spike

	−147.2° C	−142.4° C	−138.1° C	−132.8° C	−129.7° C	−125.7° C	−119.0° C	−114.5° C	−109.9° C	−99.9° C
b/a	0.736	0.747	0.743	0.728	0.742	0.738	0.757	0.739	0.746	0.758
RC_2 (sec)	4.55×10^{-4}	2.27×10^{-4}	1.22×10^{-4}	6.37×10^{-5}	3.18×10^{-5}	1.92×10^{-5}	9.37×10^{-6}	4.98×10^{-6}	2.90×10^{-6}	1.14×10^{-6}
C_2/s ($\times 10^{-11}$ F cm^{-2})	5.64	5.64	6.00	5.77	6.16	5.91	5.43	5.24	5.67	5.36
σ_{dc} (Ω^{-1} cm^{-1})	7.49×10^{-9}	1.50×10^{-8}	2.97×10^{-8}	5.53×10^{-8}	1.17×10^{-7}	1.86×10^{-7}	3.50×10^{-7}	6.35×10^{-7}	1.18×10^{-6}	2.85×10^{-6}

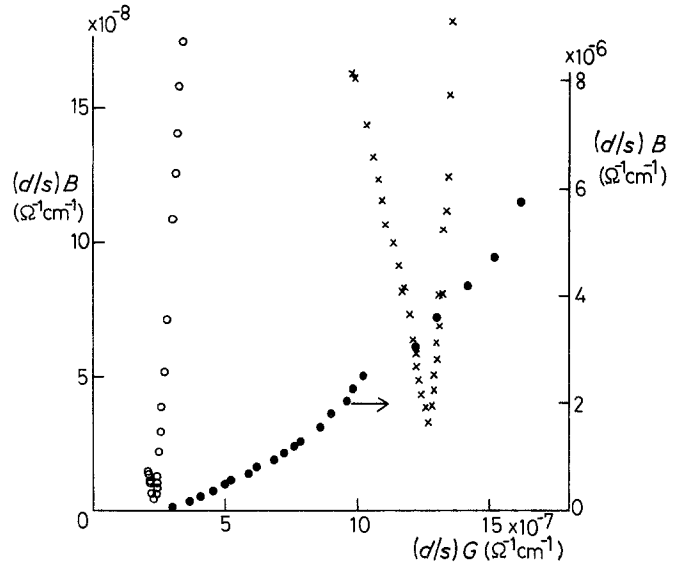

Figure 1 Complex admittance plots at −129.7° C (○, ●), and −114.5° C (×). For illustrating the absence of a semicircle within the frequency range studied, the data at −129.7° C are plotted at two different ordinates. The minima of $(d/s)B$, termed "the spikes", correspond to d.c. conductivities.

found for the Arrhenius plots of σ_{dc} (Fig. 3). The charge flowing into the cathode per half-cycle of ω_c by ionic conduction, is

$$q = \pi\sigma_{dc}E/\omega_c \quad (6)$$

where E is the r.m.s. value of the applied field. Table I shows constant values for q/E, irrespective of the temperatures used. If the anode is a totally blocking electrode and q is provided by the charge carriers within the width r of CDR, then

$$r = eq/n = \pi\sigma_{dc}E/(\omega_c en) \quad (7)$$

where n is the charge carrier density. Hence, it is expected that the width of CDR formed within the half-cycle of ω_c is almost invariant for varying temperatures.

A dielectric constant of a capacitor can be evaluated from

$$C/s = \varepsilon_1\varepsilon_0/r \quad (8)$$

if the value of r is known correctly. When 2×10^{22} cm^{-3} (the nominal density of the Ag^+ ions) is used for n, Equation 7 gives an unreasonable value of 4×10^{-12} cm for r. Therefore, in order to have a reasonable value for r, we must take into account the distribution of the charge carriers for conduction near the anode which is not so simple and abrupt as Equation 7 suggests but must be a far more slowly varying function with depth.

With decreasing temperatures the complex admittance plane no longer shows a semicircle, while concomitantly it reveals itself in the complex impedance plane (Fig. 5). Figs 6–8 show comparisons of the complex impedance and admittance plots at three different temperatures. Any semicircle in the complex impedance plane which terminates at the origin can be approximated by a parallel RC_2 circuit (Fig. 9). At the peak of the semicircle the relevant angular frequency, ω_c, satisfies the relation $\omega_c RC_2 = 1$. The spikes in the complex impedance plane correspond to d.c. conductivities as the spikes in the complex admittance plane do, as shown in Fig. 3.

Those semicircles in the complex impedance plane are also flattened to some extent, as the ratio of the short to long lengths of the semicircle indicates (Table II). Provided the peak frequency of even a distorted semicircle satisfies the relation $\omega_c RC_2 = 1$, the C_2/s values are estimated and are found to be almost temperature-independent (Table II). For constant R $(= d/(s\sigma_{dc}))$ and C_2 $(= \varepsilon_0\varepsilon_1 s/d)$ in the parallel RC_2 circuit, the relation [3]

$$(d/s)G = \sigma_{ac} = \sigma_{dc} \quad (9)$$

$$(d/s)B = \varepsilon_0\varepsilon_1\omega \quad (10)$$

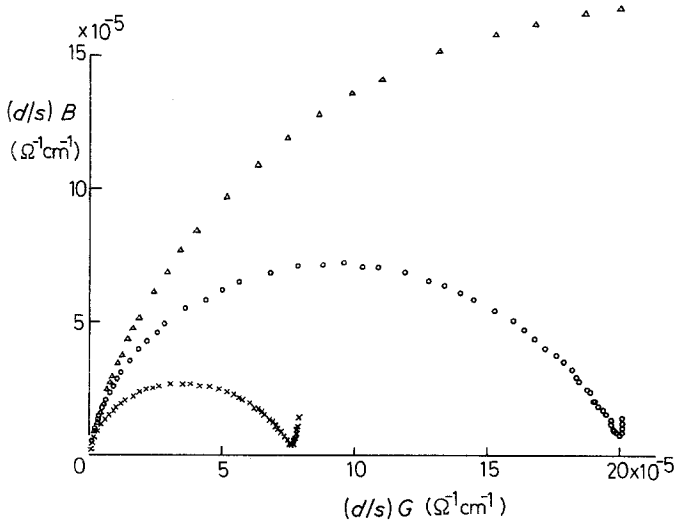

Figure 2 Complex admittance plots at −59.9° C (×), −40.2° C (○) and −20.0° C (△).

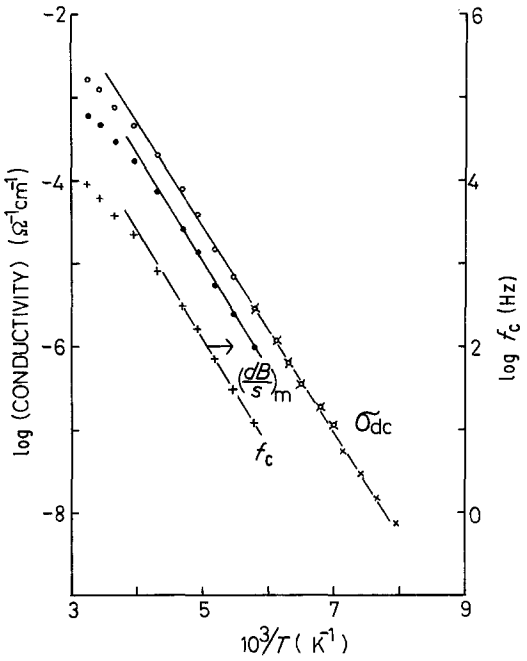

Figure 3 Arrhenius plots of d.c. conductivity, as determined from the spikes in complex admittance (○) and complex impedance (x) planes, as well as of peak maximum of dB/s, $(dB/s)_m$, and corresponding peak frequency f_c ($=\omega_c/2\pi$).

would give an ideal semicircle in the complex impedance plane. However, since our glass shows an incremental dispersion of G at high frequencies [3], the observed semicircle is flattened by a faster lowering of Z_2 ($= B/(B^2 + G^2)$) than Z_1 ($= G/(B^2 + G^2)$). The high-frequency dispersion of G was attributed [3] to the participation of ε_2, the dielectric loss factor due to dielectric relaxation of the charge carriers for conduction which is found to be a far more slowly varying function of frequency than the Debye solid.

Our glass is an Ag^+-ion conductor. The relaxation time for conduction of the Ag^+ ions, τ, is evaluated from [4]

$$\tau = (1/\nu_0) \exp(H/kT) \qquad (11)$$

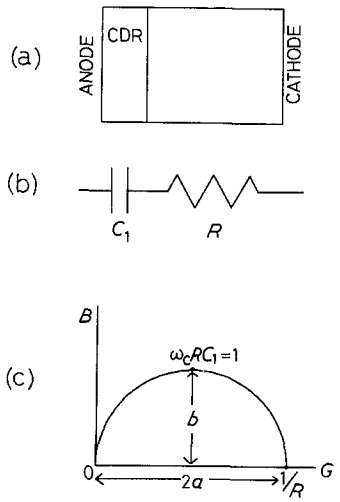

Figure 4 As conduction proceeds, the charge-carrier-depleted region (CDR) is developed near the anode (a). In this situation, the sample can be approximated by the series RC_1 circuit (b) which in the complex admittance plane is represented by a semicircle, with the peak at which the angular frequency, ω_c, satisfies the relation $\omega_c RC_1 = 1$ (c). For real glasses the semicircle is flattened to some extent, with a ratio b/a less than unity.

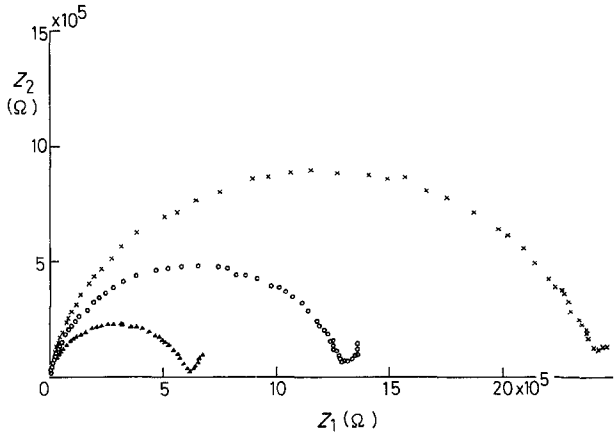

Figure 5 Complex impedance plots at −129.7°C (▲), −132.8°C (○), and −138.1°C (x).

using 3.0×10^{12} Hz for ν_0, the oscillation frequency of the Ag^+ ions [5], and 5.53 kcal mol^{-1} for H, the activation energy for conduction [1]. The Arrhenius plots of RC_2 is found to be parallel with τ, with the activation energy of 5.59 kcal mol^{-1} (Fig. 10). It is plausible in view of constant values for C_1 and C_2 that the Arrhenius plots of the time constant RC_1 also gives a parallel line, with the activation energy of 5.66 kcal mol^{-1}.

It is suggested from the previous work [3] that, at $\omega\tau \sim 1$, the dominant contribution to C_2 comes from ε_∞, the saturated value for ionic polarization of, say, the silver-iodine pairs, and $\Delta\varepsilon$, the magnitude of dielectric dispersion due to charge-carrier motion, termed conduction polarization [4], as

$$\varepsilon(\omega \sim 1/\tau) = \varepsilon_\infty + \Delta\varepsilon/2 \qquad (12)$$

From the C_2/s values listed in Table II and Equation 8, using $d = 0.0604$ cm in place of r, the ε_1 values deduced, ~41, are close to ~35 which is the estimated value from Equation 12. Similarly, C_1 would arise from conduction polarization of the oppositely charged ions (possibly the iodine ions) in CDR, as TSPC-TSDC studies of alkali silicate glass [4] suggest. Fig. 11 shows the dielectric dispersion spectra at several high temperatures, illustrating the levelling off

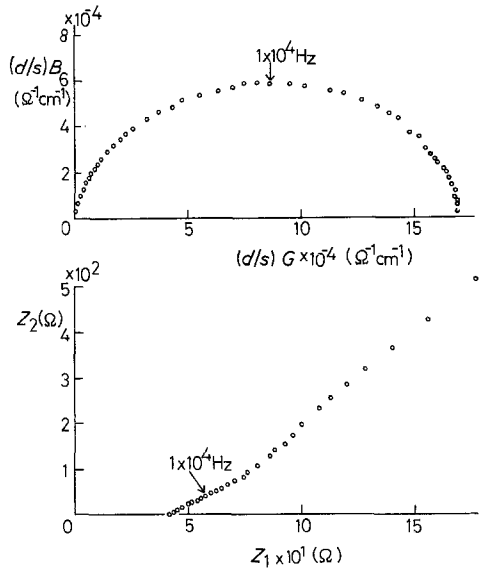

Figure 6 Complex impedance and admittance plots at +36.2°C.

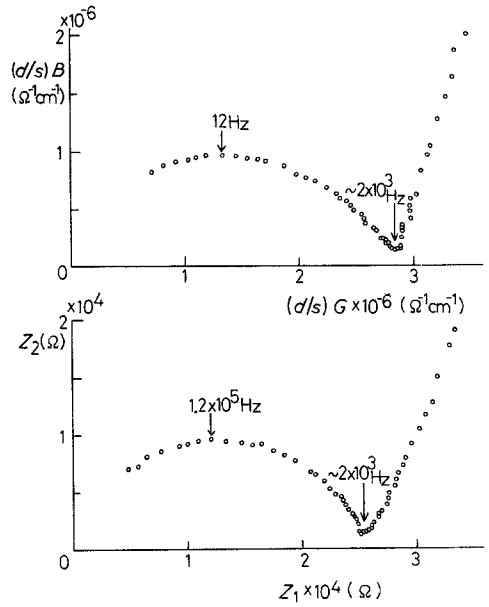

Figure 7 Complex impedance and admittance plots at −99.9° C.

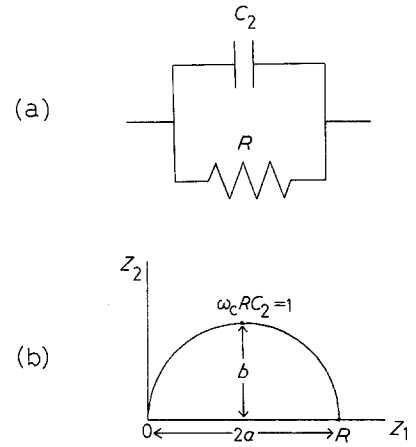

Figure 9 Parallel RC_2 circuit (a) gives a semicircle in the complex impedance plane (b). The angular frequency at the peak, ω_c, satisfies the relation $\omega_c RC_2 = 1$. For real glasses the semicircle is flattened, with the ratio b/a less than unity.

of ε_1 with as much as $\sim 8 \times 10^5$ which is 10^4 times larger than that for conduction polarization of the Ag^+ ions.

Here, use is made of the relation $\varepsilon_1 = dB/(s\omega\varepsilon_0)$. Let us discuss the validity of this derivation. Since the current precedes the applied voltage by some phase angle for both series RC_1 and parallel RC_2 circuits, the complex conductivity in response to an applied field of clockwise rotation (Equation 1) should be written as

$$\sigma^* = \sigma_1 - j\sigma_2 \quad \sigma_1, \sigma_2 \geqslant 0 \tag{13}$$

Substitution of Equations 1, 2, 4 and 13 into one of the Maxwell equations

$$\text{rot } H^* = (d/s)Y^*E^* = \sigma^*E^* + \varepsilon_0\varepsilon^*\partial E^*/\partial t \tag{14}$$

gives the universal equations [3]

$$(d/s)G = \varepsilon_0\varepsilon_2\omega + \sigma_1 \tag{15}$$

$$(d/s)B = \varepsilon_0\varepsilon_1\omega + \sigma_2 \tag{16}$$

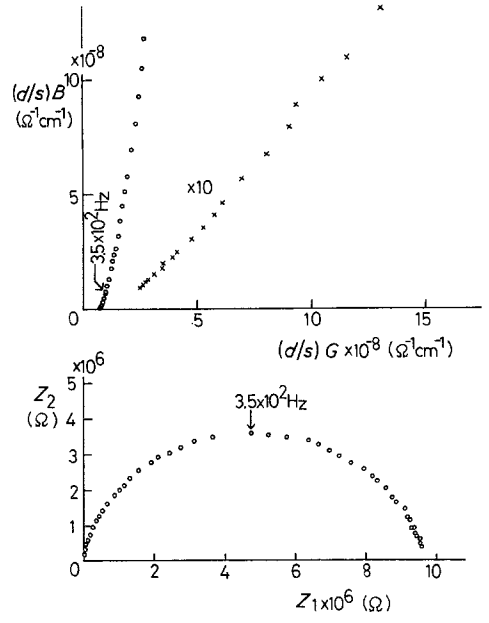

Figure 8 Complex impedance and admittance plots at −147.2° C.

At high temperatures, where the complex admittance plots show the semicircle, the Arrhenius plots of the peak maximum of dB/s, $(dB/s)_m$, and the corresponding peak frequency, f_c $(=\omega_c/2\pi)$, are found to be almost parallel to that of the d.c. conductivity (Fig. 3). With reference to Equation 16, it means that the σ_2 term is negligible and ε_1 is temperature independent at the peak frequencies. For example, the frequency dependences of ε_1 $(=dB/(s\omega\varepsilon_0))$, dB/s, and Z_1 as measured at 1.0° C are shown in Fig. 12. Since Z_1 changes little from σ_{dc} $(=7.44 \times 10^{-4}\,\Omega^{-1}\,\text{cm}^{-1})$ at frequencies above 1×10^4 Hz, the deteriorating effect of CDR or C_1 on ionic conduction is negligible in this frequency range. Nevertheless, the ε_1 value as deduced from $dB/(s\omega\varepsilon_0)$ is already up to 4×10^4. At frequencies less than f_c, ε_1 almost levels off. A slight upward deflection of ε_1 at lowermost frequencies, as observed at high temperatures (Fig. 11), may be due to the participation of σ_2. Therefore, within the frequency range measured, the contribution of σ_2 to B seems to be negligible and our derivation of ε_1 from $dB/(s\omega\varepsilon_0)$ may be valid.

Fig. 13 shows the normalized plots of G as a function of frequency, with the reference frequency f_r chosen at the dG/s value which is 10% of $(\sigma_{dc})_{spike}$ $(=dG_0/s)$. If the levelling off of ε_1 means the establishment of an ideal capacitor at CDR, G must converge

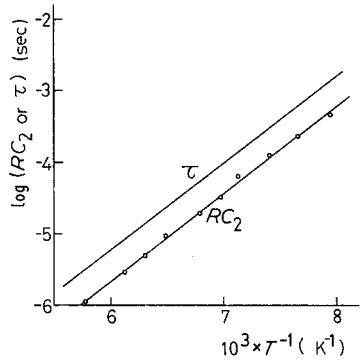

Figure 10 Arrhenius plots of RC_2, as estimated from the peaks of the semicircles in the complex impedance plane using the relation $\omega_c RC_2 = 1$, as well as of τ, the relaxation time for conduction of the Ag^+ ions.

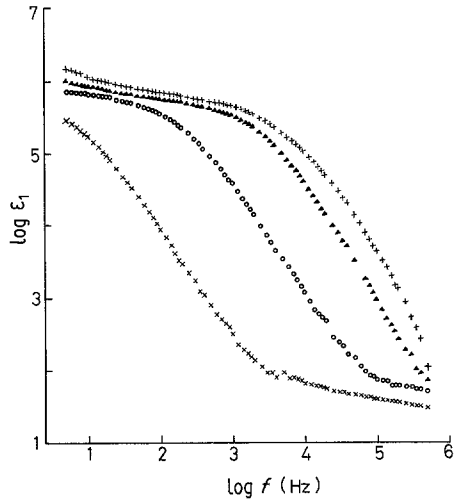

Figure 11 Dielectric dispersion spectra at several high temperatures. (x −99.9° C, o −59.9° C, ▲ +10° C, + +36.2° C)

to an absolute zero mho. Therefore, the bending of G at lowermost frequencies (Fig. 13) implies the existence of the conduction current in CDR, in support with the conduction polarization model for the origin of C_1 rather than with the double-layer model.

It is noteworthy that, even if the sample can be represented by the series RC_1 circuit, the conductivity should not be deduced simply from $R\ (=Z_1)$ using the relation $\sigma = (d/s)(1/R)$ or the dielectric constant from $C\ (=1/(\omega Z_2))$ using the relation $\varepsilon_1 = (d/s)(C/\varepsilon_0)$. The reason is that, although the admittance Y^* is a linear combination of two physical quantities (the conduction current and the displacement current in the frequency domain), the impedance Z^* is defined as a reciprocal of Y^*, that is, as a measure of resistance to the current flow, so that the expression for Z^* becomes complex, as

$$Z_1 = R = \frac{G}{G^2 + B^2} = \frac{d}{s}\frac{\varepsilon_0\varepsilon_2\omega + \sigma_1}{(\varepsilon_0\varepsilon_2\omega + \sigma_1)^2 + (\varepsilon_0\varepsilon_1\omega + \sigma_2)^2} \quad (17)$$

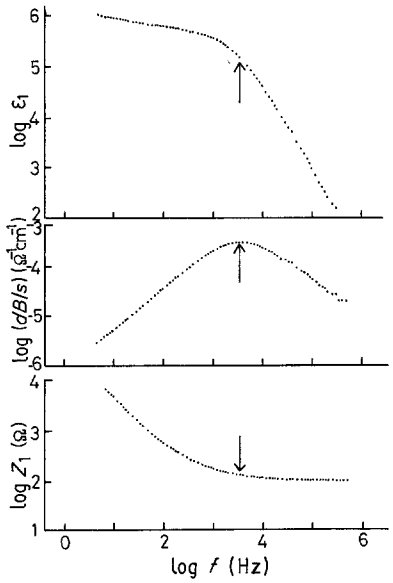

Figure 12 Frequency dependences of ε_1, as deduced from $dB/(s\omega\varepsilon_0)$, dB/s, and Z_1 at +1.0° C. Arrows indicate positions of dB/s maximum.

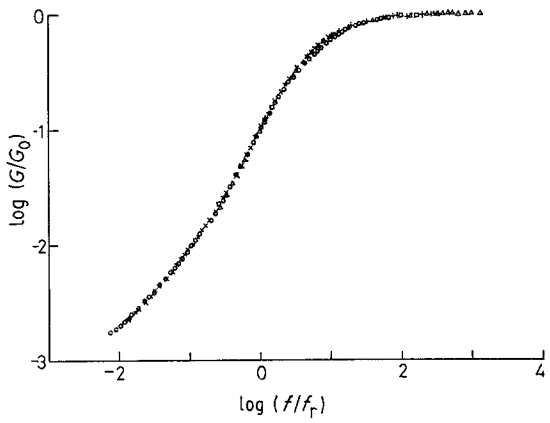

Figure 13 Normalized plots of G as a function of frequency in the temperature range from −69.8 to +36.2° C, where the reference frequency f_r is chosen at the frequency at which dG/s is 10% of $(\sigma_{dc})_{spike}$ $(=dG_0/s)$.

$$Z_2 = \frac{1}{C\omega} = \frac{B}{G^2 + B^2} = \frac{d}{s}\frac{\varepsilon_0\varepsilon_1\omega + \sigma_2}{(\varepsilon_0\varepsilon_1\omega + \sigma_2)^2 + (\varepsilon_0\varepsilon_2\omega + \sigma_1)^2} \quad (18)$$

The constancy of C_1 and C_2 seems, at a first glance, to be contradictory to the conduction polarization model because, on this model, the magnitude of polarization should decrease with increasing temperatures as

$$P = \Delta\varepsilon\varepsilon_0 E = \frac{ne^2\lambda^2 E}{\alpha kT} \quad (19)$$

where λ is the jump distance and α the number of possible jump directions of the charge carriers for conduction. In order to meet the requirement for constant C_1 and C_2, therefore, n must change in proportion to the temperature. To our knowledge, there has previously been no systematic study on the temperature-dependence of $\Delta\varepsilon$ by the difficulty in isolating $\Delta\varepsilon$ for C_2 from the overlapping contribution from C_1 or in attaining saturation of $\Delta\varepsilon$ for C_1. However, several reports [6–9] on the peak magnitude of ε_2 $(\varepsilon_{2(peak)} = \Delta\varepsilon/2$ for a system with single relaxation time) or of the electric modulus, $M_2\ (=\varepsilon_2/(\varepsilon_1^2 + \varepsilon_2^2))$, suggest an infralinear or negligible dependence of them on the reciprocal temperature. Our hypothesis of $n \propto T$ agrees, at least qualitatively, with the fact [10] that, although $M_{2(peak)}$ is almost constant below T_g [7, 9], it decreases even faster than the reciprocal temperature above T_g. This implies that the overall charge carriers become mobile in the molten state and n no longer is temperature dependent, except for the effect of dilation. The bending down of the Arrhenius plots of σ_{dc} at high temperatures (Fig. 3) suggests an attainment of saturation for n, by which the pre-exponential factor for σ_{dc},

$$(\sigma_{dc})_0 = \frac{ne^2\lambda^2\nu_0}{\alpha kT} \quad (20)$$

decreases with an increase in temperature. Rough estimate of the value for σ_{dc} at RT gives $\sim 10^{-3}\,\Omega^{-1}\,\text{cm}^{-1}$, in fair agreement with the observation (Fig. 3). Temperature-independence of $(\sigma_{dc})_0$ is

found also for the 25 $(x\mathrm{Na_2O} \cdot (1 - x)\mathrm{K_2O})5\mathrm{Al_2O_3} \cdot 70\mathrm{SiO_2}$ glasses [11].

3. Conclusion

In summary, it is concluded that at low temperatures the sample can be approximated by a parallel RC_2 circuit, with the capacitance C_2 as introduced by the constant ε_∞ due to ionic polarization of, say, the silver–iodine pairs, as well as by the relaxation process of the Ag^+ ions for conduction. At high temperatures, the development of CDR near the anode affords the sample to be approximated by a series RC_1 circuit, with C_1 as arising from CDR. Because of the very narrow width and therefore very large effective field of CDR, the C_1 values are found to be more than 10^4 times larger than those for C_2. The almost temperature independence of C_1 and C_2 suggest that, at least in ion-conducting glasses, n would increase linearly with the temperature.

Acknowledgement

The author is indebted to Dr J. Kawamura, Hokkaido University, for permission to use his original data for the $(\mathrm{AgI})_{75}(\mathrm{Ag_4P_2O_7})_{25}$ glass.

References

1. J. KAWAMURA and M. SHIMOJI, *J. Non-Cryst. Solids* **79** (1986) 367.
2. A. DOI, *J. Mater. Sci. Lett.* **6** (1987) 648.
3. *Idem, J. Appl. Phys.* **63** (1988) 121.
4. *Idem, J. Mater. Sci.* **22** (1987) 761.
5. K. FUNKE, *Solid State Ionics* **3–4** (1981) 45.
6. R. J. CHARLES, *J. Amer. Ceram. Soc.* **46** (1963) 235.
7. V. PROVENZANO, L. P. BOESCH, V. VOLTERRA, C. T. MOYNIHAN and P. B. MACEDO, *ibid.* **55** (1972) 492.
8. H. NAMIKAWA, *J. Non-Cryst. Solids* **18** (1975) 173.
9. R. J. GRANT, M. D. INGRAM, L. D. S. TURNER and C. A. VINCENT, *J. Phys. Chem.* **82** (1978) 2838.
10. F. S. HOWELL, R. A. BOSE, P. B. MACEDO and C. T. MOYNIHAN, *ibid.* **78** (1974) 639.
11. C. T. MOYNIHAN, D. L. GAVIN and F. SYED, *J. Phys., Colloq.* **C9** (1982) 395.

Received 2 February
and accepted 1 June 1988